Z-2

PICOSECOND REFLECTOMETRY TECHNIQUE FOR ON-CHIP CHARACTERIZATION OF MILLIMETER-WAVE SEMICONDUCTOR DEVICES

Christen Rauscher

Naval Research Laboratory
Washington, DC 20375-5000

Abstract — A multi-sampler reflectometer technique is described for on-chip characterization of semiconductor devices at millimeter-wave frequencies. Focus is on enhancing measurement accuracy and frequency band coverage by augmenting photoconductive circuit elements, which perform signal generation and sampler functions, with pulse-shaping and impedance-matching networks. The approach is illustrated with a GaAs 150 GHz bandwidth example.

INTRODUCTION

The design of high-frequency semiconductor circuits for optimum performance critically depends on the accuracy with which the terminal characteristics of individual devices can be assessed. The implied need for reliable measurements becomes increasingly difficult to accommodate as system applications expand up into the millimeter-wave regime. Several of the difficulties encountered are related to the predominant reliance on measurement system front-ends that employ hollow waveguide components. Such systems are inherently band limited, causing inconvenience when measuring over wide frequency ranges. Of main concern, however, are the interfaces between the hollow waveguide components and the semiconductor chip to be tested. Although measurement errors arising from the transitional discontinuities theoretically can be corrected for, the approach often fails to inspire confidence in practice. Additional problems occur when attempting to characterize active devices, as they experience purely reactive port terminations at frequencies below waveguide cut-off, potentially giving rise to uncontrolled oscillations.

A way to overcome the limitations is to adopt an approach in which the high-frequency front-end portion of the measurement system is monolithically integrated with the device or subcircuit to be tested on the same semiconductor chip. By relying on quasi-TEM signal propagation throughout the composite monolithic structure, the troublesome discontinuities between device and measurement system front-end are avoided, and concerns over possible low-frequency oscillations due to waveguide cut-off are dispersed. Optical techniques provide an elegant means for implementation of such an on-chip measurement concept. Foremost among applicable techniques are those which utilize photoconductive effects and those which are based on exploitation of electro-optic phenomena. Common to each approach is the need for a high-speed laser to generate a train of short light pulses, with the required lasing wavelength determined by the particular approach under consideration.

The technique outlined in the following employs photoconductive circuit elements, so-called PCEs, in a time-domain-reflectometer-type configuration. Fast-switching PCEs are thereby not only used to carry out sampling functions, but also used to generate trains of short electromagnetic pulses that provide incident signal waveforms with sufficient millimeter-wave frequency content. The underlying basic idea of using PCEs for signal generation and sampling is well documented in the literature [1],[2]. The current investigation aims at demonstrating the significant performance benefits to be derived from the introduction of various circuit- and system-related concepts.

APPROACH

In the case of one-port measurements, the underlying concept referenced above involves basically a section of uniform transmission line deposited on the semiconductor substrate, with the device under test connected to one end of the line, a dc-biased high-speed PCE connected to the other end, and one additional PCE used to tap the interconnecting line at some midway point. The biased PCE is excited with a train of very fast laser pulses spaced a few nanoseconds apart. The typical PCE response to excitation by a laser pulse consists of a sharp rise in conductance followed by a more gradual exponential relaxation. The risetime is controlled by the light pulse and the carrier pairs it generates in the semiconductor material, whereas the decay time constant is determined by the carrier recombination process. A train of high-speed electromagnetic signal pulses is consequently launched onto the transmission line. The incident signal pulses, and subsequently the pulsed reflection responses of the test device, are then sampled with the help of the other PCE. Its gating operation is controlled by a derivative of the original train of laser pulses, with this derivative subjected to variable time delay. The effective sampling aperture thereby mirrors the aforementioned time dependence of the PCE conductance.

Fundamental to this time-domain-based concept is the need to reliably differentiate between incident and reflected signal waveforms on the transmission line, as this directly impacts the accuracy with which the characteristics of the device under test can be assessed. The basic approach, as described in the literature and outlined above, tacitly assumes that incident and reflected pulses are sufficiently separated in time to yield adequate differentiation with the help of a single sampling element. In situations like the one presently considered, where efficient utilization of available wafer area is important, this requirement becomes difficult to satisfy. The current approach overcomes this constraint by utilizing more than one sampling element to tap the transmission line at specified intervals. The additional measurement information thus obtained allows accurate identification of incident and reflected waveforms regardless of cross-contamination of signals at the points of observation.

Implementation of the multiple-sampler concept reduces the issue of measurement accuracy to that of achievable time resolution. The remaining principal constraints are the relaxation time constants of the PCEs, and parasitic circuit-related effects. Time

constants for GaAs in the vicinity of one picosecond have been accomplished through localized radiation damage to the semiconductor material [3]. The focus here is on further improvements in resolution and accuracy to be obtained through the use of pulse-shaping networks in conjunction with the PCEs. A functional block diagram of the composite on-chip measurement system is depicted in Fig. 1. This example contains one pulse generation PCE and three sampler PCEs, with the respective pulse-shaping networks labeled G and S.

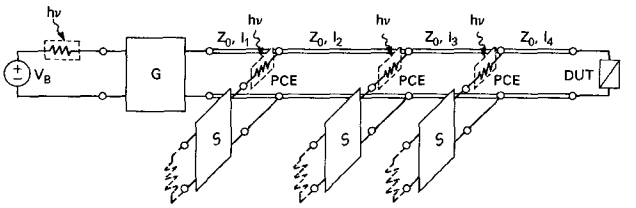

Fig. 1 — Functional block diagram of on-chip multiple-sampler reflectometer.

Conception and design of photoconductor-based on-chip measurement tools have, in the past, been based in the time domain. However, due to strict periodicity, all signals involved may also be conveniently represented by Fourier series expansions. This, in turn, permits both system design and signal analysis to be carried out in the frequency domain. Even though the sampling operation itself is time-based and is most easily dealt with in the time domain, this consideration is outweighed by the advantages of working in the frequency domain. One prominent advantage is the applicability of established network synthesis techniques and RF measurement concepts. Within the context of the present investigation, this advantage has been systematically exploited in the design of signal generation and sampler circuits for optimum performance, in the dealings with parasitic circuit effects, in the formulation of signal acquisition needs, and in the processing of measurement-derived signal information.

SIGNAL GENERATION

As mentioned earlier, the signal incident on the main transmission line of the reflectometer system consists of a train of sharp pulses. The pulse repetition frequency, f_p, coincides with that of the controlling laser and typically lies in the vicinity of 100 MHz. For the purposes of the present discussion, it shall be assumed that the conductance $g_p(t)$ of the pulse-generating PCE can be expressed as

$$g_p(t) = \hat{G}_p \cdot e^{-t/\tau_p}, \quad N \cdot \frac{1}{f_p} \leq t < (N+1) \cdot \frac{1}{f_p} \qquad (1)$$

with $\hat{G}_p$ the peak conductance of the radiation-damaged PCE, and τ_p the associated carrier recombination time constant. Neglecting parasitic circuit effects for the time being, the incident voltage on the line, $V_{\text{inc}}(f)$, represented in the frequency domain, is given by

$$V_{\text{inc}}(f) \approx V_B \cdot R_0 \cdot \hat{G}_p \cdot f_p \cdot \tau_p \cdot \sum_{n=-\infty}^{+\infty} \left\{ \delta(f - nf_p) \cdot \sum_{k=0}^{+\infty} \frac{(-R_0 \cdot \hat{G}_p)^k}{k + 1 + j2\pi n f_p \tau_p} \right\}. \qquad (2)$$

For $1/\hat{G}_p$ considerably smaller than the characteristic transmission line impedance R_0, only the lowest order term in the summation over k need be retained. The frequency spectrum of the incident voltage thus consists of individual components spaced f_p apart with a low-pass-type amplitude envelope that drops off at a rate of 6 dB per octave beyond the critical frequency

$$f_c = \frac{1}{2\pi\tau_p}. \qquad (3)$$

The principal task of network G in Fig. 1 is to provide a high-end boost to the frequency spectrum (2) of the incident pulse train. The network is also tasked with compensation for parasitic reactance effects that will accompany any physical implementation of a PCE. An example of such a network is given in terms of its schematic circuit diagram in Fig. 2. It is designed for microstrip implementation on a GaAs substrate and consists of four transmission line segments of characteristic impedance $Z_0 = 100\ \Omega$, two resistors valued $R_1 = 75\ \Omega$ and $R_2 = 25\ \Omega$, respectively, a via hole inductance L_v, and some capacitive fringing effects. The radiation-damaged PCE, for which a decay time constant of two picoseconds is assumed, is connected to the input port of the pulse-shaping network through a blocking capacitor and a via hole. The calculated spectral envelope (solid line) characterizing the composite signal generator is shown in Fig. 3. Also depicted, for comparison, is the response to be observed when relying on the conventional approach (dashed line) in which the PCE is directly connected to the main transmission line and to an additional segment of line that acts as resistive shunt ballast. As is evident from the figure, the 3-dB roll-off point has been pushed upward in frequency by a full octave, providing spectral coverage up through 160 GHz with only a modest increase in overall circuit complexity.

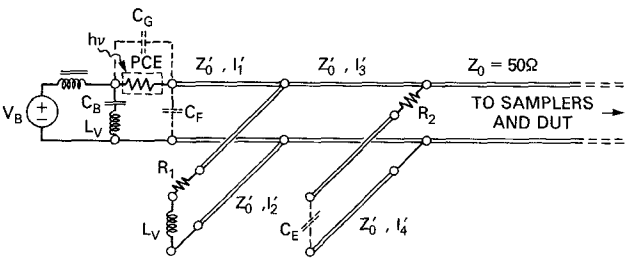

Fig. 2 — Equivalent circuit diagram of PCE pulse generator with pulse-shaping network.

SAMPLER CIRCUIT

The second topic focused on is the design of the sampler structures. Emphasis, thereby, is on minimizing the effective sampling gate aperture and on minimizing parasitic perturbation of incident and reflected signals on the main transmission line. This is accomplished through employment of low-pass two-port networks S, as indicated in Fig. 1, that couple the secondary terminals of the sampler PCEs to the instrumentation tasked with recording the low-frequency sampler output signals. Figure 4 depicts a schematic diagram of a microstrip sampler circuit designed for a two-picosecond switching PCE identical to the one assumed in Fig. 2. The circuit contains one segment of 100 Ω transmission line, a 200 Ω series resistor, a blocking capacitor, and a via hole connection to ground.

In contrast to the previously discussed pulsed incident signal generation, where the application of the time-based pulse-shaping concept was conveniently dealt with in the frequency domain alone, the analytical considerations surrounding the sampler tend to be more complicated. This is due to the fact that the sampling process not only involves the primary incident and reflected signals with their harmonically related spectral components spaced f_p

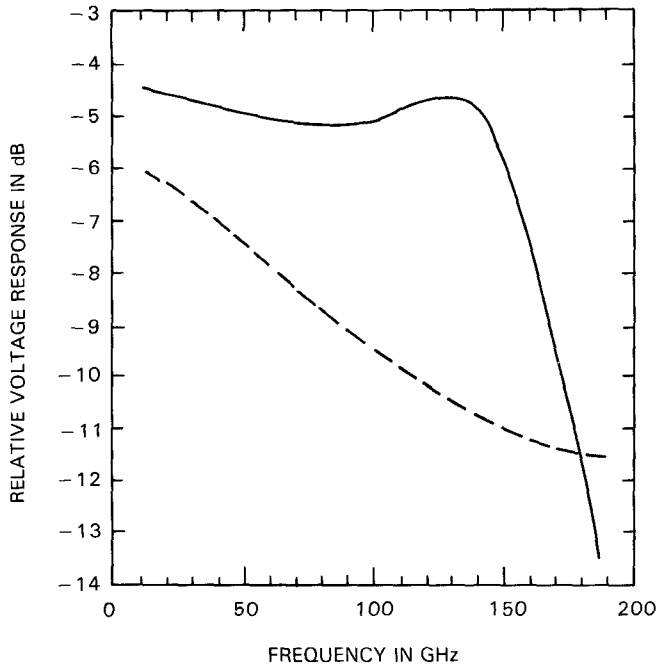

Fig. 3 — Calculated envelope response of pulse generator frequency spectrum: ——with pulse-shaping network, - - - without pulse-shaping network.

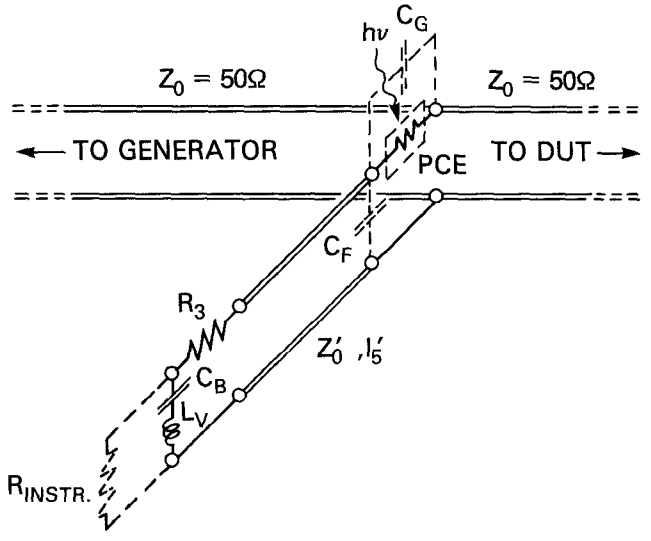

Fig. 4 — Equivalent circuit diagram of PCE sampler structure.

apart, but also the sampling function with its harmonic components spaced $f_s < f_p$ apart, as well as all the additional components spaced $\Delta f = f_p - f_s$ apart that are generated in the process. Sampler operation is described in the frequency domain by

$$V_l(f) \cdot Y_l(f) = G_s(f) * [V(f) - V_l(f)] + Y_s(f) \cdot [V(f) - V_l(f)] \quad (4)$$

with V the voltage on the main line to be measured at the particular point of sampling, V_l the voltage at the input of network S (Fig. 1), and Y_l the input admittance of S, while G_s and Y_s represent the effective PCE conductance and parasitic reactance properties, respectively. The task is to solve for the line voltage components $V(nf_p)$, $n = 0, 1, \ldots$, based on knowledge of the measured baseband response of $V_l(n\Delta f)$, $n = 0, 1, \ldots$, as recorded at the secondary port of low-pass network S. Despite the formal simplicity of (4), finding the general solution is a very formidable assignment. This is due to the simultaneous presence of the convolution operator $(*)$ related to the time-windowing effect of the basic sampling process, and of the multiplication operator $(\cdot)$ related to the frequency-windowing effects of the various circuit elements and parasitics. In practical situations, $Y_l(f)$ will be orders of magnitude larger than $G_s(f)$ at respective harmonics of f_p. This follows from the necessity to insure that the voltage sensed by the sampler PCE be a truthful replica of the voltage V on the main line. Application of this assumption, together with a few other practical considerations, permits an explicit solution to be derived

$$V(nf_p) = \left[1 + \frac{Y_s(nf_p)}{Y_l(nf_p)}\right] \cdot \frac{Y_l(n\Delta f)}{G_s(-nf_s)} \cdot V_l(-n\Delta f), \quad n = 0, 1, 2, \ldots \quad (5)$$

Similarly, the effective shunt admittance Y_{eff} presented to the main transmission line by the composite sampler circuit at harmonics of f_p can be written as

$$Y_{\text{eff}}(nf_p) = [Y_l^{-1}(nf_p) + Y_s^{-1}(nf_p)]^{-1}, \quad n = 0, 1, 2, \ldots \quad (6)$$

Although these last two expressions constitute approximations, they are accurate to within one permill under practical circumstances.

REFLECTOMETER SYSTEM

The third issue to be addressed is the necessity to employ multiple sampler structures for adequate differentiation between incident and reflected signals that travel on the main transmission line and partially overlap in time. Two appropriately positioned sampler circuits, in principle, can provide all the information required to solve for the spectral components of each of the two signals. However, this type of reflectometer cannot resolve signal components at frequencies where the two observation points are spaced by multiples of half a wavelength. The spacing of the sampler must hence be selected in accordance with requirements for frequency band coverage. An alternative is to utilize more than two samplers to fill in the voids.

Figure 5 depicts the microstrip layout of a three-sampler on-chip reflectometer designed for a 100-μm-thick GaAs substrate. It comprises a pulse generating network to the left, a 50 Ω transmission line leading up to a 25 Ω test termination, and three samplers positioned along the line at unequal intervals for optimum frequency band coverage up through 150 GHz. The entire structure possesses a length of 2.5 mm. Both the generator circuit and the sampler structures constitute implementations of the previously defined solutions. It may be noted, in particular, how relatively little space the generator pulse-shaping network actually occupies,

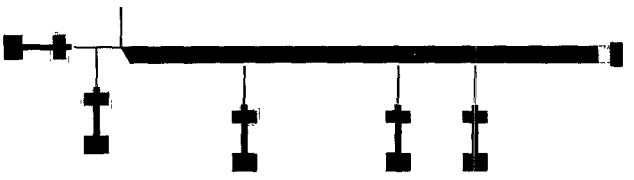

Fig. 5 — Microstrip lay-out of 5-to-150-GHz on-chip reflectometer on a 100-μm-thick GaAs substrate. The circuit contains one pulse generator sub-circuit, three sampler sub-circuits, a 25 Ω load, and a connecting main 50 Ω transmission line.

when compared to the quite significant performance benefits derived from it.

To further illustrate the technique, the time-domain response of the system to the 25 Ω test load has been simulated on the computer. The signal observed by the number two sampler circuit has been plotted in Fig. 6, together with the initiating conductance modulation response of the generator PCE. Of special interest is the pronounced multi-frequency ringing exhibited by the incident pulse signal as it propagates past the sampling point beginning at 12 picoseconds. This ringing is introduced by the generator pulse-shaping network and is responsible for boosting the spectral content of the incident waveform at the high end of its frequency range, as discussed earlier. The reflection signal stemming from the 25 Ω load and its series via hole inductance is observed by the number two sampler circuit beginning at 27 picoseconds.

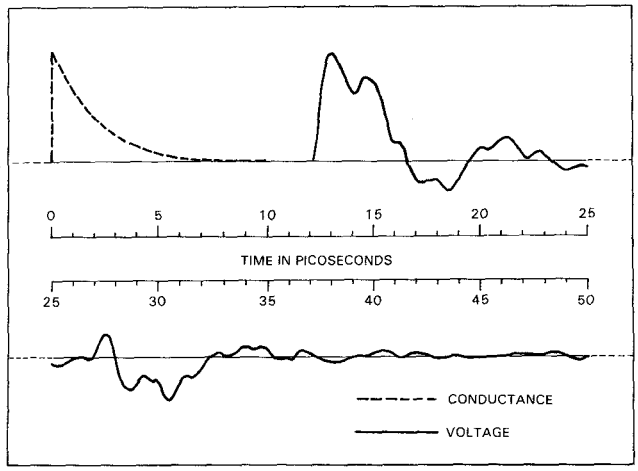

Fig. 6 — Signal response observed by the number two sampler circuit (solid line), together with the conductance response of the generator PCE (dashed line).

CONCLUSIONS

Of the various optical techniques potentially applicable to RF device characterization, the photoconductor-based approach has been pursued here in detail. A principal advantage of this approach is that only dc-type probe connections between chip and supporting instrumentation are required, as all RF signal functions—including incident signal generation—are performed entirely on-chip. The objective of the current investigation has been to focus on key factors responsible for restricting frequency band coverage and measurement accuracy. The designated solution that has evolved, based on assessment of these factors, encompasses the use of multiple sampling points positioned along the main transmission line, and the incorporation of special pulse-shaping and impedance-matching networks. These features provide reliable identification of incident and reflected signals, as well as significantly enhanced performance of PCEs serving as high-speed pulse generators and sampling gates. The millimeter-wave design example used for illustration highlights the comparatively modest circuit-related effort involved in a typical implementation of the approach.

Acknowledgement — The author wishes to acknowledge many helpful discussions with Drs. R. B. Hammond of the Los Alamos National Laboratory and B. A. Auld of Stanford University.

REFERENCES

[1] D. H. Auston, "Impulse response of photoconductors in transmission lines," Vol. QE-19, April 1983.

[2] W. R. Eisenstadt, R. B. Hammond, and R. W. Dutton, "On-chip picosecond time-domain measurements for VLSI and interconnect testing using photoconductors," IEEE Trans. El. Dev., Vol. ED-32, Feb. 1985.

[3] R. B. Hammond, personal communication.